Journal of GeoEngineering, Vol. 10, No. 2, pp. 63-73, August 2015
http://dx.doi.org/10.6310/jog.2015.10(2).4

LESSONS LEARNED IN DESIGN OF AN EXCAVATION WITH THE INSTALLATION OF BUTTRESS WALLS

Pio-Go Hsieh [1*], Chang-Yu Ou [2], Yung-Kuang Lin [3], and Fang-Chih Lu [4]

ABSTRACT

Installation of buttress walls is one of the auxiliary measures for the protection of adjacent buildings during excavation in Taiwan. But only a few complete case studies with buttress walls have been found in the literature. This study performs a case study regarding the design of an excavation with the installation of buttress walls. Before excavation, a preliminary prediction concerning the diaphragm wall deflection was implemented using an empirical method and the three-dimensional finite element method. Based on the preliminary prediction, the buttress walls were designed. Then the diaphragm wall deflections were predicted again and the efficiency of the buttress walls was evaluated. During excavation, the prediction was modified following the actual field observation. Based on the results of the observation and prediction, a numerical analysis model was established and the efficiency of the buttress walls was investigated.

Key words: Excavation, buttress wall, diaphragm wall deflection, case study, prediction.

1. INTRODUCTION

The buildings and public facilities are often intensive in urban areas due to limited land resources. The need for using underground space is increasingly rapid. In addition to an increase in excavation depth, new excavation projects are often close to adjacent properties. However, diaphragm wall deflection and ground settlement normally occur as a result of excavation. Excessive ground settlement frequently damages adjacent properties in urban areas. To avoid the damage of adjacent properties during excavation, it is necessary to adopt auxiliary measures prior to excavation to limit the diaphragm wall deflection and ground settlement. Though the integrity of adjacent buildings can be protected by underpinning, it is not practical to underpin a large number of target buildings, either from a financial or political point of view. Therefore, reducing excavation induced movements to a tolerable amount by auxiliary measures is a viable alternative. Strengthening the bracing system and/or installing the cross wall or increasing the passive resistance in excavation zone are commonly adopted auxiliary measures in engineering practice, and case histories with varying degrees of success have been reported (Wong *et al*. 1987; Gaba 1990; Hsieh *et al*. 2003; Liu *et al*. 2005; Parashar *et al*. 2007; Ou *et al*.2011; Hsieh *et al*. 2013).

Recently, buttress walls have been used as alternative auxiliary measures for protection of adjacent buildings during excavation in Taiwan. Basically, buttress walls are concrete walls constructed from one side of the diaphragm wall to a certain length prior to excavation, as shown in Fig. 1. They are usually cast with the diaphragm wall at the same time.

According to the experiences of practicing engineers, buttress walls seem to have a good effect in reducing the deflection of diaphragm walls. Although buttress walls have been applied in many excavations, research on complete case studies of excavation with buttress walls is rather deficient. Only a few studies on buttress walls have been found in the literature. Hsieh and Lu (1999) introduced a simple model for preliminary design of buttress wall. Lin and Woo (2007) studied a deep excavation with buttress walls and concluded that three-dimensional numerical analysis is necessary to represent the real behavior of diaphragm wall deflection. Hwang *et al*. (2007) investigated the field observations of an excavation with buttress walls and concluded that based on the same diaphragm wall deflection, it needs thicker thickness of diaphragm wall if the excavation was not installed with the buttress wall. Chen *et al*. (2011) examined the influence of the geometry of the buttress walls on the displacement of buttressed diaphragm wall by performing three-dimensional finite element analysis. Hsieh *et al*. (2013) performed a series of parametric studies, including the length and thickness of buttress

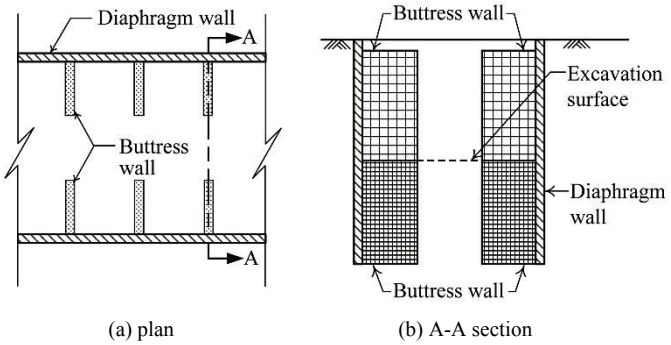

Fig. 1 Schematic diagram of buttress wall (a) plan (b) A-A section

Manuscript received March 12, 2015; revised July 23, 2015; accepted July 29, 2015.

[1] Professor (corresponding author), Department of Assets and Property Management, Hwa Hsia University of Technology, New Taipei City, 23568, Taiwan (e-mail: spg@cc.hwh.edu.tw).
[2] Professor, Department of Civil and Construction Engineering, National Taiwan University of Science and Technology, Taipei, 10672, Taiwan.
[3] President, Ground Master Construction Co., LTD., Taipei, 10689, Taiwan.
[4] General Manager, Ground Master Construction Co., LTD., Taipei, 10689, Taiwan.

walls for the effect of buttress walls and concluded that the effects of buttress walls in reducing wall deflection mainly come from the surface friction of the buttress walls. The longer buttress walls length, the better efficiency in reducing the wall deflection. Increase of the buttress wall length has a prominent effect in reducing wall deflection than that of the buttress wall thickness. All of these studies indicated that buttress walls have certain effects in reducing the deflection of diaphragm walls.

This study performs a case study of an excavation with the installation of buttress walls. Before excavation, a preliminary prediction concerning diaphragm wall deflection was done using an empirical method and the three-dimensional finite element method for the excavation without buttress walls. Based on the preliminary prediction results, the buttress walls were designed. Then the diaphragm wall deflections were predicted for first prediction and the efficiency of the buttress walls was evaluated. During excavation, the first prediction results were compared with the field observation and the corrective prediction was implemented based on the real construction condition. A numerical analysis model was established by comparing the diaphragm wall deflections between the corrective prediction and field observation. The efficiency of the buttress walls was also investigated through the comparison of the results obtained from three-dimensional finite element analysis.

2. THE CASE HISTORY

The studied project, situated in the Taipei geological T2 subzone (Huang *et al*. 1987), was a 38-story structure with a seven-level basement. As shown in Fig. 2, the excavation was 64 m in length and 43 m in width, and surrounded by five buildings: A 18-story and 15 year old building with 6-level basement 4 m away from the excavation area in the east side; a 12-story and 10 year old building with 4-level basement and three less than 5-story and over 20 year old buildings, 4 m away from the excavation area in the north side. The west and south side of the excavation were adjacent to 30 m and 40 m main roads with heavy traffic, respectively.

As indicated by site investigation, the basic soil properties, strength properties and compression properties obtained via boring and laboratory testing are shown in Fig. 3. The subsoil is comprised of six alternating layers of clayey and sandy soils above the silty gravel located below GL (ground surface level) −39.6 m. From top to bottom, they are described as follows:

1. The 1st layer, from the ground surface to GL −5.0 m, except a backfill together with gravels and sundries with thickness about 0.4 m to 1.4 m, it is a layer of yellow brown mixed gray silty clay of a total unit weight (γ_t) about 18.44 kN/m^3, average natural water content (ω) between 28% and 51%, void ratio (e) between 0.91 and 1.09, liquid limit (LL) between 35 and 45, plasticity index (PI) between 15 and 23, compression index (C_c) 0.4, swelling index (C_s) 0.04, effective friction angle (ϕ') 28°.
2. The 2nd layer, in the range of GL −5.0 m to GL −15.9 m, is a layer of gray silty sand, occasionally mixed with thin clayey silt, with the standard penetration number (N values) varying from 5 to 17. Its γ_t is about 19.42 kN/m^3, ω between 19% and 32% and $\phi' = 30°$.

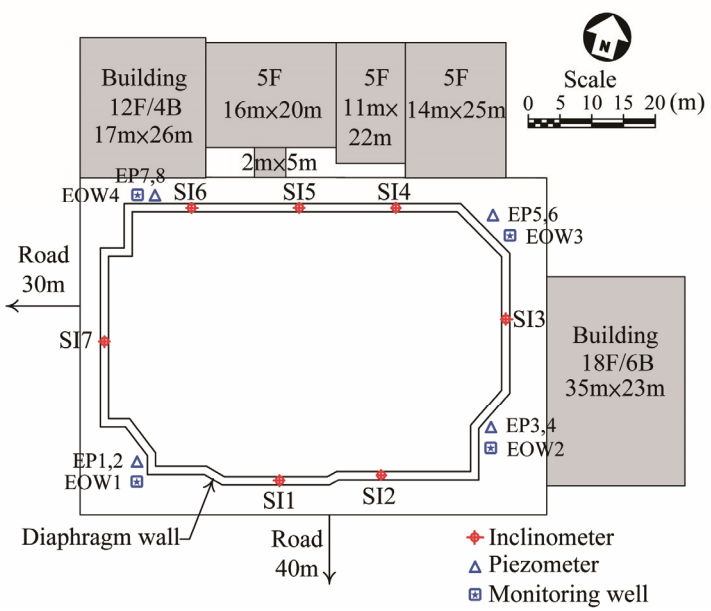

Fig. 2 Excavation geometry and instrumentation

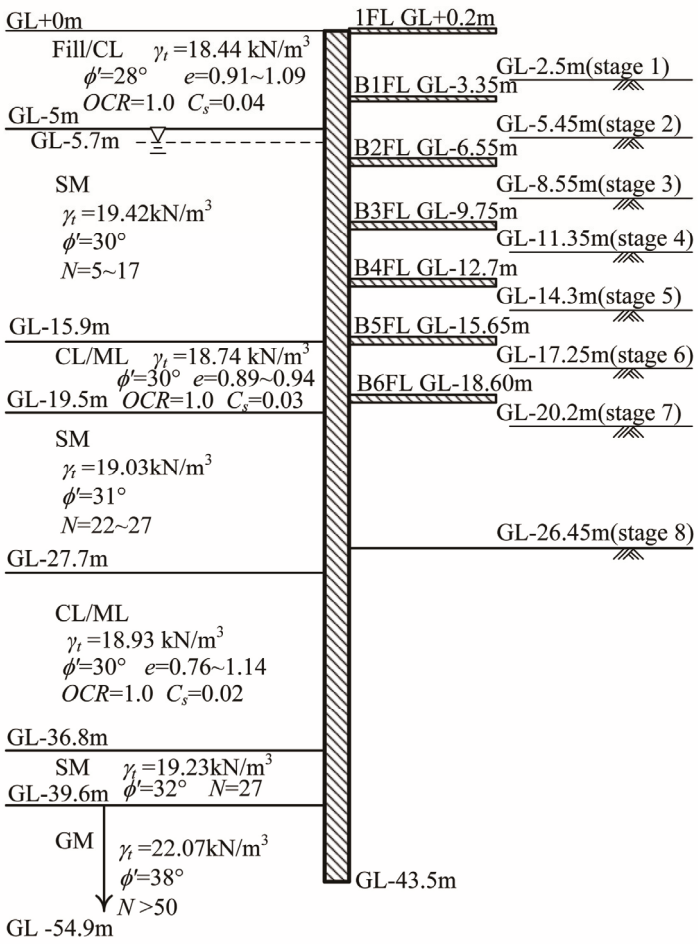

Fig. 3 Profile of construction sequence and subsurface soil layers

3. The 3rd layer, from GL −15.9 m to GL −19.5 m, is a layer of gray silty clay, clayey silt, occasionally mixed with thin silty sand. Its γ_t is about 18.74 kN/m^3, ω between 24% and 37%, *e* between 0.89 and 0.94, *LL* between 29 and 38, *PI* between 5 and 14, $C_c = 0.3$, $C_s = 0.03$ and $\phi' = 30°$.
4. The 4th layer, from GL −19.5 m to GL −27.7 m, is a layer of gray silty sand, occasionally mixed with thin sandy silt, with N values varying from 22 to 27. Its γ_t is about 19.03 kN/m^3, ω between 19% and 32%, $\phi' = 31°$.
5. The 5th layer, from GL −27.7 m to GL −36.8 m, is a layer of gray silty clay, clayey silt, occasionally mixed with thin silty sand. Its γ_t is about 18.93 kN/m^3, ω between 23% and 40%, *e* between 0.76 and 1.14, *LL* between 28 and 40, *PI* between 3 and 18, $C_c = 0.2$, $C_s = 0.02$ and $\phi' = 30°$.
6. The 6th layer, from GL −36.8 m to GL −39.6 m, is a layer of gray silty sand, mixed with thin sandy silt, with *N* values about 27. Its γ_t is about 19.23 kN/m^3, ω between 18% and 29%, $\phi' = 32°$.
7. The 7th layer, from GL −39.6 m to GL −54.9 m, is a layer of gravel, mixed with gray silty sand, with *N* values larger than 50. Its γ_t is about 22.07 kN/m^3, $\phi' = 38°$.

The groundwater level is locates at GL −5.7 m, but the piezometric water level in the 4th layers (sandy soil) is about GL −9.2 m and those in the 6th layers (sandy soil) and 7th layer (gravelly soil) are about GL −18.1 m.

A 1.3 m thick diaphragm wall was used as the earth retaining structure. The depth of the diaphragm wall was 43 m, penetrating 3.9 m into gravel layer. The design compressive strength of the concrete (f_c') was 27.5 MPa. The basement was constructed using the top-down construction method up to 26.45 m in depth. The concrete floor slabs, designed with 27.5 MPa of the f_c', of the basement were treated as a lateral support system during excavation. According to Fig. 3, the excavation was completed in 8 stages, which are described as

1. Excavated down to GL −2.5 m.
2. Constructed the girder-plates of the floor slab (1FL) with 0.25 m in thickness at GL +0.2 m and then excavated down to GL −5.45 m.
3. Constructed the girder-plates of the floor slab (B1FL) with 0.25 m in thickness at GL −3.35 m and then excavated down to GL −8.55 m.
4. Constructed the girder-plates of the floor slab (B2FL) with 0.4 m in thickness at GL −6.55 m and then excavated down to GL −11.35 m.
5. Constructed the flat slabs of the floor slab (B3FL) with 0.4 m in thickness at GL −9.75 m and then excavated down to GL −14.3 m.
6. Constructed the flat slabs of the floor slab (B4FL) with 0.4 m in thickness at GL −12.7 m and then excavated down to GL −17.25 m.
7. Constructed the flat slabs of the floor slab (B4FL) with 0.4 m in thickness at GL −15.65 m and then excavated down to GL −20.2 m.
8. Constructed the flat slabs of the floor slab (B6FL) with 0.4 m in thickness at GL −18.6 m and then excavated down to GL −26.45 m.

To monitor the diaphragm wall deflection, 7 inclinometers (SI1 ~ SI7) with 45 m in depth were installed penetrating 5 m into gravel layer to keep the bottom located at a fixed position. Among them, inclinometer SI1 was damaged at the beginning of excavation so their data were excluded in this study. Inclinometers SI-3 and SI-4 remained functional until stage 8 and the monitored values at all stages except for stage 8 were employed for study. In addition, the monitoring wells and piezometers in silty sand were installed at the corner outside of the excavation, as shown in Fig. 2.

As shown in Fig. 2, the east and north of excavation were contiguous to five buildings and the west and south contiguous to a main road with heavy traffic. Therefore based on the regulation (Taiwan Geotechnical Society 2001), the allowable value of maximum surface settlement (δ_{vm}) induced by excavation was set to be 30 mm.

The relationship between δ_{vm} and the maximum diaphragm wall deflection (δ_{hm}) for excavations in Taipei has been established by Hsieh and Ou (1998) as follows:

$$\delta_{vm} = (0.5 \sim 0.75)\ \delta_{hm} \tag{1}$$

where the upper limit is mostly for clay, the lower limit for sand and those for the alternating layers of sand and clay fall in between the two limits. For very soft clay, the δ_{vm} may be large than 1.0 δ_{hm} in some cases.

Therefore Eq. (1) was used to evaluate the controlled value of δ_{hm} for this studied project. Since the sandy soils were the predominant strata in the site, as shown in Fig. 3, the δ_{vm} was evaluated by 0.6 δ_{hm}. Accordingly, the controlled value of δ_{hm} for the studied project was set as 50 mm.

3. PRELIMINARY PREDICTION

The empirical method and three-dimensional finite element analysis were employed to predict the diaphragm wall deflection. The prediction results from these two methods were compared with each other to establish rationality and accuracy of the prediction, which will be taken as a basis for protecting the adjacent buildings.

3.1 Prediction Using Empirical Method

In the preliminary prediction, the maximum diaphragm wall deflection induced by excavation was estimated following Ou *et al*. (1993) and Ou *et al*. (1996). According to Ou *et al*. (1993), the maximum diaphragm wall deflection under the plane strain condition ($\delta_{hm,ps}$) in the Taipei area can be predicted by the following relationship:

$$\delta_{hm,ps} = (0.2\% \sim 0.5\%)\ H \tag{2}$$

where *H* is the final excavation depth; the upper limit is mostly for clay, the lower limit for sand and those for the alternating layers of sand and clay fall in between the two limits.

In addition, Ou *et al*. (1996) presented the concept of three-dimensional diaphragm wall deflection affected by the corner effect and defined the plane strain ratio (*PSR*) as:

$$PSR = \frac{\delta_{hm,d}}{\delta_{hm,ps}} \tag{3}$$

where $\delta_{hm,d}$ is the maximum diaphragm wall deflection at a distance d to the corner.

Figure 4 shows relationship between *PSR* and aspect ratio for excavations as established by Ou *et al*. (1996).

In the preliminary prediction, Eqs. (2), (3) and Fig. 4 were adopted to estimate the maximum diaphragm wall deflection of the studied project. Since the sandy soils were the predominant strata in the studied project, as shown in Fig. 3, the $\delta_{hm,ps}$ for the excavation was estimated by 0.3% H and to be 79.4 mm. As shown in Fig. 2, the aspect ratios (B/L = 43/64, where the definition of B and L can be referred to Fig. 4) of the studied project was equal to 0.67. By referring to Fig. 4, the corresponding *PSR* value for the section of SI5 locating at central sections of the long excavation sides were estimated as 0.92. Therefore, the maximum diaphragm wall deflection at the section of SI5 was evaluated as 73.1 mm. Obviously this value exceeds the controlled value of δ_{hm}.

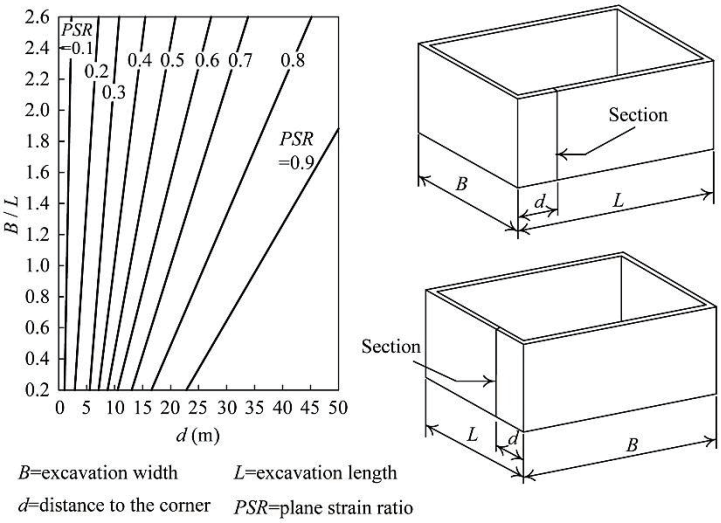

Fig. 4 Relationship between plane strain ratio and aspect ratio for excavations

3.2 Prediction Using Three-Dimensional Finite Element Analysis

As previously mentioned, the predicted δ_{hm} from the empirical method obviously exceeded the controlled value. The three-dimensional finite element analysis was performed to further predict the diaphragm wall deflection. A three-dimensional finite element computer program, PLAXIS 3D (2013), was used as a basic analysis tool. The hardening soil model (Schanz *et al*. 1999), referred to as the HS model, was adopted to simulate the behavior of soils, including clayey soil and sandy soil/ gravel under the undrained and drained conditions, respectively.

Of the HS parameters, the unit weight of soil (γ_t), effective cohesion (c') and the effective internal friction angle (ϕ') can be obtained from the laboratory. The angle of dilatancy (ψ) can be approximated by $\psi = \phi' - 30°$ for sandy soil. However, the ψ is mostly equal to zero for ϕ' less than 30°. The Poisson's ratio for the unloading-reloading state (v_{ur}) can be reasonable assumed to be 0.2 and the failure ratio (R_f) is set equal to 0.9. The coefficient of the at-rest earth pressure for sandy soil (K_0), can be obtained using the equation (Jaky 1944):

$$K_0 = 1 - \sin\phi' \tag{4}$$

The K_0 value for clay can be obtained according to Ladd *et al*. (1977) as:

$$K_{0,OC} = K_{0,NC}(OCR)^{\alpha} \tag{5}$$

where $K_{0,OC}$ is the coefficient of at-rest earth pressure for over-consolidated soils with over-consolidation ratio, OCR; α is the empirical coefficient, which can be approximated by $\alpha = \sin\phi'$; $K_{0,NC}$ is the coefficient of the at-rest earth pressure for normally consolidated clay. According to Hsieh (1993), the relationship in normally consolidated clay between $K_{0,NC}$ and ϕ' is close to Jaky's equation (Eq. (4)), therefore $K_{0,NC}$ can be estimated through Eq. (4).

In addition, the HS model also requires the secant stiffness (E_{50}^{ref}) corresponding to the reference stress, p^{ref}, the tangent referential stiffness for primary oedometer loading (E_{oed}^{ref}), the unloading/reloading referential stiffness (E_{ur}^{ref}) and the power for stress-level dependency of stiffness (m). These parameters were often evaluated from the correlations because they are not easily obtained directly from conventional laboratory or field tests. In this analysis, p^{ref} = 100 kPa. For clay, m is set equal to 1.0, and E_{ur}^{ref} can be estimated according to Lim *et al*. (2010) as:

$$E_{ur}^{ref} = \frac{3(1+e)p^{ref}(1-2\nu_{ur})}{C_s/\ln 10} \tag{6}$$

where e is the initial void ratio and C_s the swelling index.

E_{50}^{ref} and E_{oed}^{ref} can be obtained by the following equation suggested by Calvello and Finno (2004):

$$E_{50}^{ref} = \frac{E_{ur}^{ref}}{3} \tag{7}$$

$$E_{oed}^{ref} = 0.7E_{50}^{ref} \tag{8}$$

As for sandy soil, E_{50}^{ref}, E_{ur}^{ref} and E_{oed}^{ref} can be estimated according to Khoiri and Ou (2013) as:

$$E_{50}^{ref} = \frac{E_s}{3\left(\frac{\sigma_3'}{p^{ref}}\right)^m} \tag{9}$$

$$E_{ur}^{ref} = 3E_{50}^{ref} \tag{10}$$

$$E_{oed}^{ref} = 1.5E_{50}^{ref} \tag{11}$$

where E_s is the Young's modulus under σ_3' corresponding to the soil in the field; σ_3' is the effective horizontal stress. Khoiri and Ou (2013) back analyzed excavation case histories and found $E_s \approx (2000 \sim 3000)N$, where N is the standard penetration numbers. In this study, the lower bound of E_s was adopted (E_s = 2000N) and m is set equal to 0.5.

Moreover, the silty gravel soil exists at this site around GL –45 m. Deng (2013) has found from back analysis that E_{ur}^{ref} was about 256 MPa, $E_{50}^{ref} \approx 85$ MPa and $E_{oed}^{ref} \approx 85$ MPa.

Table 1 summaries the parameters of the soils used in the analysis.

The structural members such as diaphragm walls and concrete floor slabs employed in the top-down construction method were plate elements and simulated as linear elastic material. The Poisson's ratio for concrete is set equal to 0.15. The Young's modulus of concrete (E_c) was estimated according to the suggestion by ACI Committee 318 (1995) as:

$$E_c = 4700\sqrt{f_c'} \tag{12}$$

where f_c' is the 28-day compressive strength of concrete (MPa).

Table 2 summaries the parameters of the structure used in the analysis, in which the E_c of concrete was reduced by 20%, considering construction effects (Ou 2006). In analysis, the interface property (R_{int}) between the diaphragm wall and the adjacent soil was set as rigid ($R_{int} = 1.0$).

Figure 5 shows the finite element mesh used for the preliminary prediction. The depth of mesh was set at 54.9 m, considering that hard rock would not deform during excavation. Since the analysis just focused on diaphragm wall deflection rather than ground settlement, the horizontal boundaries were set at the distance two times the final excavation depth from the diaphragm wall. The finite element model was therefore 169.8 m in length and 148.8 m in width. The analysis followed the exact construction procedure (as displayed in Fig. 3), excavation geometry, retaining-support system and in-situ water level. Dewatering was performed before each excavation. The water level inside the excavation was lowered to the excavation surface when excavation was conducted in clayey soil, and lowered to 1 m below the excavation surface when in sandy soil.

Table 1 Soil parameters

(a) Undrained layers											
Depth (m)	γ_t (kN/m^3)	c' (kPa)	ϕ' (°)	ψ (°)	C_s	e_0	E_{ur}^{ref} (kPa)	E_{50}^{ref} (kPa)	E_{oed}^{ref} (kPa)	m	ν_{ur}
0-2	18.44	0	28	0	0.04	0.91	19794	6598	4619	1.0	0.2
2-5	18.44	0	28	0	0.04	1.09	21660	7220	5054	1.0	0.2
15.9-17.7	18.74	0	30	0	0.03	0.89	26116	8705	6094	1.0	0.2
17.7-19.5	18.74	0	30	0	0.03	0.94	26807	8936	6255	1.0	0.2
27.7-30	18.93	0	30	0	0.02	0.95	40418	13473	9431	1.0	0.2
30-32	18.93	0	30	0	0.02	1.14	44356	14785	10350	1.0	0.2
32-34	18.93	0	30	0	0.02	0.87	38759	12920	9044	1.0	0.2
34-36.8	18.93	0	30	0	0.02	0.76	36480	12160	8512	1.0	0.2
(b) Drained layers											
Depth (m)	γ_t (kN/m^3)	c' (kPa)	ϕ' (°)	ψ (°)	SPT-N Value	E_{ur}^{ref} (kPa)	E_{50}^{ref} (kPa)	E_{oed}^{ref} (kPa)	m	ν_{ur}	
5-7	19.42	0	30	0	5	15543	5181	7771	0.5	0.2	
7-9	19.42	0	30	0	12	33606	11202	16803	0.5	0.2	
9-11	19.42	0	30	0	14	35964	11988	17982	0.5	0.2	
11-13	19.42	0	30	0	17	40573	13524	20287	0.5	0.2	
13-15.9	19.42	0	30	0	14	30922	10307	15461	0.5	0.2	
19.5-22	19.03	0	31	1	22	43880	14627	21940	0.5	0.2	
22-24	19.03	0	31	1	25	47542	15847	23771	0.5	0.2	
24-27.7	19.03	0	31	1	27	48621	16207	24311	0.5	0.2	
36.8-39.6	19.23	0	32	2	27	43864	14621	21932	0.5	0.2	
39.6-54.9	22.07	0	38	8	>50	256000	85000	85000	0.5	0.2	

Table 2 Structural information and parameters

Structure	Depth(m)	t (m)	γ (kN/m^3)	E_c (MPa)	ν
Diaphragm wall	0-43.5	1.3	23.54	19718	0.2
1FL	0.2	0.25	23.54	19718	0.2
B1FL	3.35	0.25	23.54	19718	0.2
B2FL	6.55	0.25	23.54	19718	0.2
B3FL	9.75	0.4	23.54	19718	0.2
B4FL	12.7	0.4	23.54	19718	0.2
B5FL	15.65	0.4	23.54	19718	0.2
B6FL	18.6	0.4	23.54	19718	0.2
Buttress wall	0-20.2	0.6$^{\#}$, 0.8*	23.54	15573	0.2
Buttress wall	20.2-35	0.6$^{\#}$, 0.8*	23.54	19718	0.2

$^{\#}$: Buttress wall type A and B ; * : Buttress wall type C

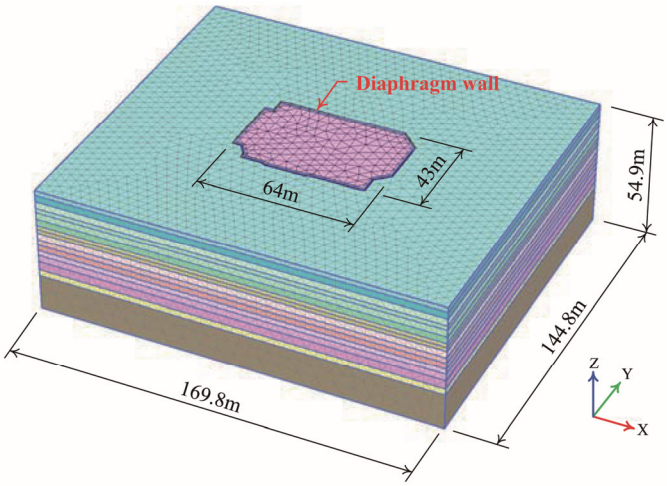

Fig. 5 Finite element mesh used for the preliminary prediction

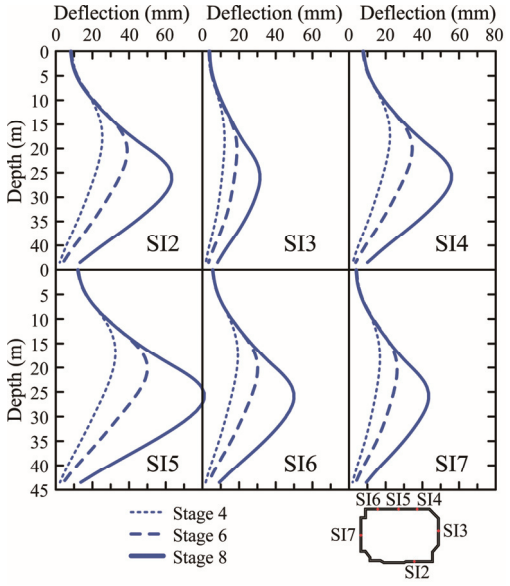

Fig. 6 Diaphragm wall deflections at stages 4, 6 and 8 obtained from the preliminary prediction using three dimensional finite element analysis

Figure 6 shows the diaphragm wall deflections at the sections of SI2 to SI7 at stages 4, 6 and 8 obtained from the preliminary prediction using three-dimensional finite element analysis. The maximum diaphragm wall deflection occurred at the section of SI5, in which the δ_{hm} at stage 8 was 80.1 mm and its corresponding δ_{hm} / H was equal to 0.3%. The result was consistent with that from empirical method (73.1 mm). Figure 6 also shows that the δ_{hm} at the sections of SI4 to SI6 and SI2, located at the north and south of the excavation zone respectively, exceeded the controlled value (50 mm). The δ_{hm} at the east and west didn't exceed, but was close to the controlled value. Since the excavation were surrounded by five buildings and main roads with heavy traffic, as shown in Fig. 2. To avoid the damage of adjacent buildings and properties during excavation, it was considered to adopt auxiliary measures prior to excavation to limit the diaphragm wall deflection and ground settlement.

4. THE FIRST PREDICTION FOR THE INSTALLATION OF BUTTRESS WALLS

Although ground improvement and cross wall are common measures to reduce the excavation-induced ground movements for protecting the adjacent buildings in excavations, the quality of ground improvement sometimes is not easy to be ensured in practice and the installation of cross walls in a wide excavation, like the studied project, is costly. Furthermore, the maximum diaphragm wall deflection in the south-north direction obtained from preliminary prediction was not very much larger than the controlled value and the maximum diaphragm wall deflections at the east and west of the excavation even did not exceed the controlled value. Only a partial protection measure was needed. Therefore the buttress wall was selected as a remedial measure for the protection of adjacent buildings and properties in the excavation.

Figure 7 shows the allocations of buttress walls in the excavation where thirteen buttress walls were adopted. Three types of buttress walls with different thickness (t_{bw}) and length (L_r) were constructed as shown in Fig. 8: Type A with the t_{bw} of 0.6 m and L_r of 5 m from GL +0 m to GL −35.0 m; Type B with the t_{bw} of

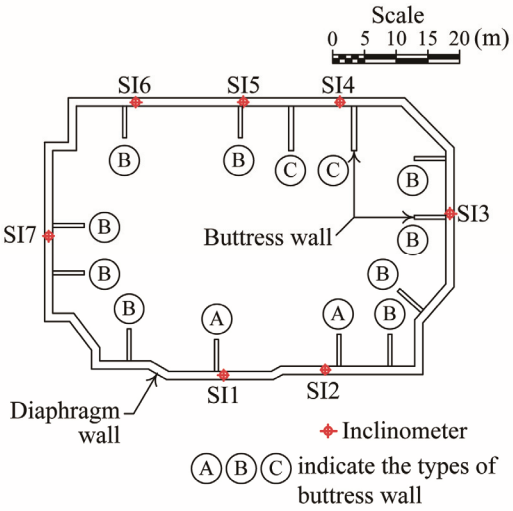

Fig. 7 Allocations of the buttress walls

0.6 m and L_r of 2.5 m from GL +0 m to GL −20.2 m, 5.0 m from GL −20.2 m to GL −35.0 m; Type C with the t_{bw} of 0.8 m and L_r of 7 m from GL +0 m to GL −35.0 m. All of the buttress walls were cast with concrete with f_c' of 13.7 MPa from GL +0 m to GL −20.2 m, 24 MPa from GL −20.2 m to GL −35.0 m. Because the buttress walls were dismantled with the process of excavation, no reinforcement steel bars were placed in the buttress walls above the final excavation depth but temperature steel bars were arranged in the buttress walls below the final excavation depth.

As shown in Fig. 3, the soil was excavated, along with the demolishment of buttress walls, to GL −2.5 m, referred to as stage 1. The concrete floor slab at the ground level (1FL) was then installed and the soil and buttress walls were excavated and demolished simultaneously down to GL −5.45 m, referred to as stage 2. The procedure was repeated until excavation down to GL −20.2 m, stage 7. After completion of stage 7, the concrete

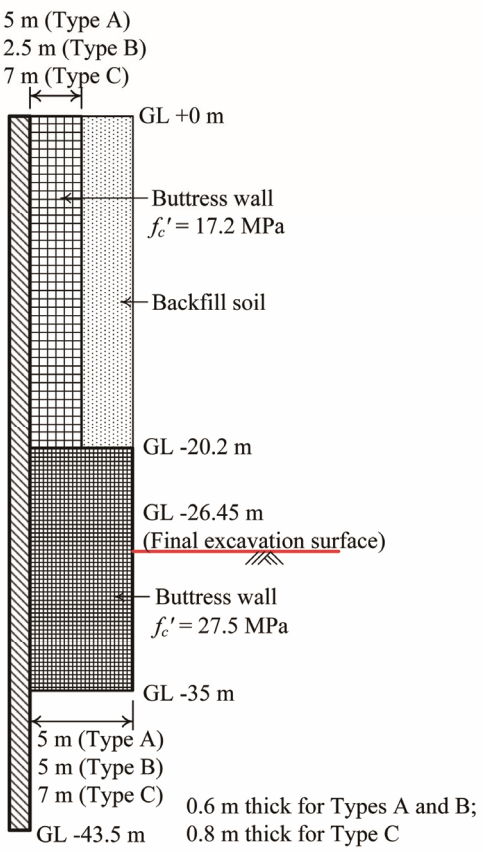

Fig. 8 Types of buttress wall used in the excavation

floor slab was constructed at GL −18.60 m (B6FL) and the soil was excavated to the final depth, GL −26.45 m, but the buttress walls were only demolished to GL −20.20 m (stage 8). At the final stage, the 0.9 m thick mat foundation was cast and then the buttress walls were demolished down to the final depth, *i.e.*, 26.45 m and the concrete floor slab (B7FL) with 0.25 m in thickness was built at GL −23.1 m.

Three-dimensional finite element analysis was used to predict the diaphragm wall deflection of the excavation with buttress wall in the first prediction. The buttress walls were simulated by plate elements with R_{int} = 1.0. The input parameters were estimated similar to that of the diaphragm wall and also summarized in Table 2. The simulation of construction procedure, parameters of the soil and structure, condition of water level and mesh were also the same as the preliminary prediction except that the positions of buttress walls in the mesh were put with the plate elements to simulate the buttress walls and that the buttress walls were demolished along with excavation at stages 1 to 7.

Figure 9 shows the diaphragm wall deflections observed at SI2 to SI7 at stages 4, 6 and 8 and those obtained from the first prediction where the excavation was allocated with buttress walls. For comparison, those obtained from the preliminary prediction (without buttress walls) is also shown in the figure. As shown in Fig. 9, with buttress walls, the diaphragm wall deflections could be reduced to a certain extent. The δ_{hm} at SI4, SI6 and SI2, located at the north and south of the excavation zone, respectively, were reduced to less than the controlled value except a little bit larger than the controlled value at SI5. The δ_{hm} at the east and west of the excavation zone were also reduced significantly to less than controlled value.

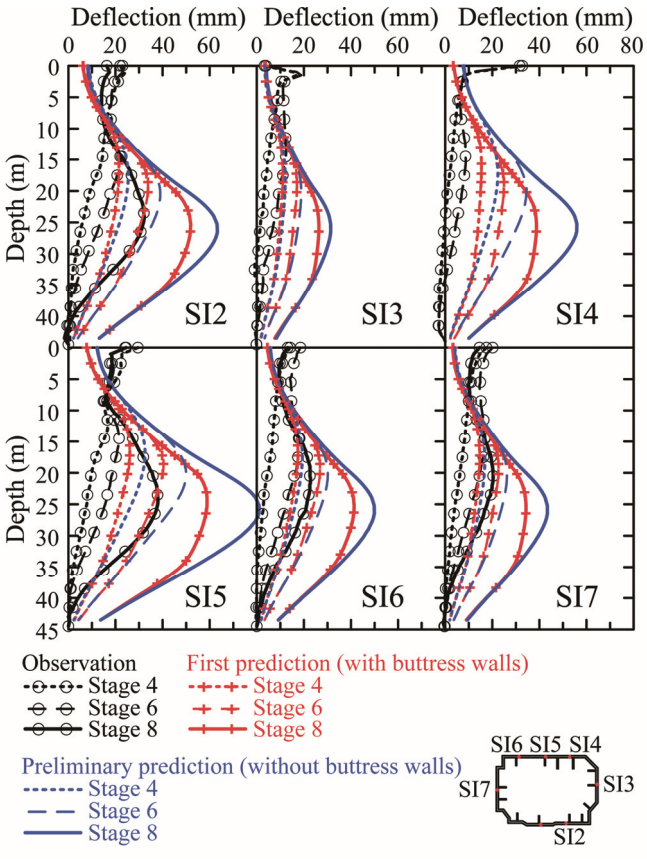

Fig. 9 Comparison of the diaphragm wall deflections at stages 4, 6 and 8 between the observation and the first prediction

For evaluating the efficiency of buttress walls in excavations quantitatively, the ratio of reduction in the maximum diaphragm wall deflection (*RRD*) is defined as：

$$RRD = \frac{\delta_{hm,nobw} - \delta_{hm,bw}}{\delta_{hm,nobw}} \times 100\% \quad (13)$$

where $\delta_{hm,nobw}$ is the maximum deflection of the diaphragm wall without buttress walls; $\delta_{hm,bw}$ is the maximum deflection of the diaphragm wall with buttress walls.

As shows in Table 3, the *RRD* values at SI4, SI5 and SI6, located in the north of the excavation zone, were equal to 30.6%, 27.6% and 17.4%, respectively. The *RRD* values at SI2, SI3 and SI7, located in the south, east and west, respectively, were equal to 20%, 16% and 22.0%. Installation of buttress walls had some effects in reducing the diaphragm wall deflection. The diaphragm wall deflections at SI5 and SI7 with buttress walls were moderately smaller than those without buttress walls. Their *RRD* values were 26.9% and 23.9%, respectively. Installation of buttress walls had a moderate effect in reducing the diaphragm wall deflection.

When excavation was executed in practice, the diaphragm wall deflections obtained from the first prediction were generally consistent with those from observation at stages 1 to 3. However, the predicted results were overestimated at stage 4, as shown in Fig. 9. Figure 9 also shows the observations at stages 6 and 8, in which there were no observations at SI3 and SI4 at stage 8 because the location of SI-3 was planned to be a material stacking area at the time when excavation at stage 8 and the inclinometer tube of SI4 was blocked at stage 7. Since the diaphragm wall deflections obtained from the first prediction before excavation was obviously overestimated, prediction needed to be corrected.

5. CORRECTIVE PREDICTION

As mentioned previously, the diaphragm wall deflections obtained from the first prediction were overestimated after stage 4. Although the observed diaphragm wall deflections were still smaller than the predicted ones and also within the controlled value, the possible reasons of overestimation were explored and the corrective prediction was implemented to understand the overall diaphragm wall deflection behavior.

Many factors such as the simulation of excavation, constitutive model of soils, parameters of the structures and soils, water level and adjacent buildings may affect the wall deflection. Since the constitutive model of structure and soils employed in this study has been verified by Lim *et al*. (2010) and Khoiri and Ou (2013), the effects of other factors on the wall deflection were thus investigated through a series of three dimensional parametric studies. In each analysis, the computed wall deflections were compared with the field observation. It was found that the main differences came from the simulation of the adjacent building and water level within the excavation zone. Field inspection also confirmed that these two factors in the aforementioned analyses were not realistically close to construction environment. These two main differences and their consideration in the subsequent corrective prediction are described as follows:

1. Simulation of the adjacent buildings

As shown in Fig. 2, five adjacent buildings, 4 m away from the excavation zone in the east and north side, were not considered in the first prediction. Table 4 shows the information of these adjacent building, including foundation type, depth of foundation (D_f), depth (H_t) and thickness (t_{dw}) of diaphragm wall used in these adjacent building, thickness (t) of basement floor slab and foundation slab, and loading applied to foundation plate (Q).

Since the loading of these buildings were transmitted to the beams, then to the columns, and then spread to the foundation slabs, the weight of the buildings and their loading was assumed to uniformly act on the foundation slabs. For the buildings with individual footings, all of the footings were assumed to act on a plate at GL −2m and then the uniform total loading was directly applied on it, as shown in Fig. 10(a). For the building with mat foundations, the diaphragm wall, basement floor slabs and foundation slabs were configured at their position and corresponding depth, and the soils was assumed to remain in the basement, the uniform net loading was directly applied on the foundation slabs, as shown in Fig. 10(b).

Since those adjacent buildings were more than 10 years old, the excess pore water pressure induced by the loading of those buildings was assumed to fully dissipate. When performing the corrective prediction, the adjacent buildings were constructed and loading was applied with the full dissipation of excess pore water pressure in each clay layer after calculating the initial stress.

2. Water level within the excavation zone

The water levels inside the excavation zone were set the same as those outside before excavation in the preliminary prediction and the first prediction where the groundwater level was set at GL −5.7 m, and the water level in sandy/gravelly soil located at the 4th and 6th as well as 7th layers were set at GL −9.2 m and GL −18.1 m, respectively. However, in actual construction, to avoid the trench collapse of the diaphragm wall construction, the ground water level was usually lowered during trench excavation until construction of the diaphragm wall was completed.

Table 3 Maximum wall deflections and *RRD* values obtained from the first prediction and the corrective prediction

No.	Side	First prediction			Corrective prediction		
		$\delta_{hm,nobw}$ (mm)	$\delta_{hm,bw}$ (mm)	*RRD* (%)	$\delta_{hm,nobw}$ (mm)	$\delta_{hm,bw}$ (mm)	*RRD* (%)
SI2	South	63.3	51.0	19.4	43.9	36.2	17.5
SI3	East	31.4	26.4	16.0	16.7	13.8	17.4
SI4	North	55.9	38.8	30.6	31.9	26.1	18.2
SI5	North	80.1	58.0	27.6	52.7	38.5	27.0
SI6	North	50.0	41.3	17.4	27.6	22.9	17.0
SI7	West	44.0	34.3	22.0	30.9	23.5	24.0

Table 4 Information of the adjacent buildings

Story/ basement	Age (year)	Area (m^2)	Foundation type	D_f (m)	H_t (m)	t_{dw} (m)	t^+ (m)	Q^+ (kPa)
18F/6B	15	35 × 23	Mat foundation	22	39	1.1	0.25	71.58*
12F/4B	10	17 × 26	Mat foundation	16	33	0.8	0.25	23.8*
5F/0B	> 20	16 × 20	Footing	2	–	–	0.25	49.05#
5F/0B	> 20	11 × 22	Footing	2	–	–	0.25	49.05#
4F/0B	> 20	14 × 25	Footing	2	–	–	0.25	39.24#

+: Assessed value; ∗: Net loading; #: Total loading

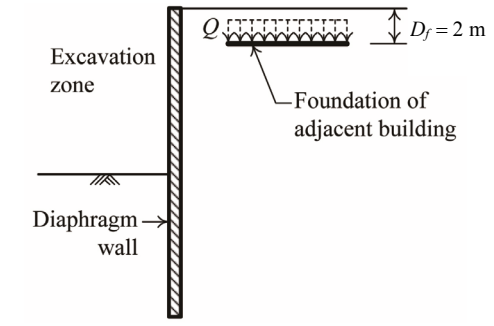

(a) With footing foundation

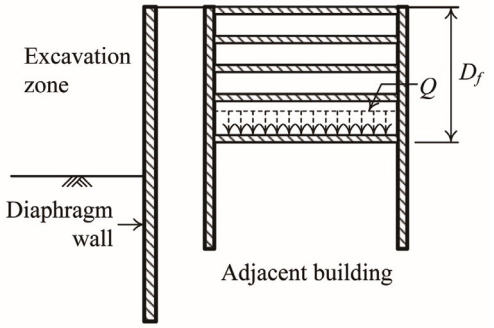

(b) With mat foundation

Fig. 10 Simulation of the adjacent building

Although the water levels outside the excavation zone would be affected during the construction of the diaphragm wall, the groundwater would be replenished from the surrounding after the completion of the diaphragm wall construction. The water levels would recover to the original level, which would be the same as that at the time of site investigation. The observation obtained from the monitoring wells and piezometers at the corner of the outside of the excavation (Fig. 2) also verify this phenomenon. However, the groundwater inside the excavation zone could not be replenished due to the fact that the impermeable diaphragm wall prevented the water replenish from the outside into the excavation zone and that the wall penetrated through the silty clay located at the 3rd and 5th layer, as shown in Fig. 3. Under such condition, the silty sand located at the 2nd and 4th layers would remain about zero water pressure. This presumption was confirmed by the field construction record that dewatering was not conducted in the first 4 stages, even not proceeded in the subsequent stages to the completion of excavation, the excavated soils exhibited much less water content than the initial one. It was therefore justified that the water level inside the excavation zone was not the same as those outside.

When executing the corrective prediction, first considered that the excess pore water pressures in clay generated by the adjacent buildings was completely dissipated, the diaphragm walls and buttress walls were constructed, then the water level in the 2nd and 4th layers of silty sand inside the excavation zone were set at GL −27.7 m. Excavation was then simulated after the nodal displacements of the mesh were reset to 0.

Figure 11 shows the comparison of diaphragm wall deflections between the observation and the corrective prediction with buttress wall at SI2 to SI7 at stage 4. The diaphragm wall deflections at the subsequent stages 6 and 8 were also shown in the figure.

Compared diaphragm wall deflections from the corrective prediction with those from the first prediction (Figs. 11 and 9), the corrective prediction was much more close to the observation at each stage. At excavation stage 4, except for SI4 where the wall deflection was larger than the field observation, the diaphragm wall deflections from the corrective prediction were generally consistent with the observation. At the subsequent stages 6

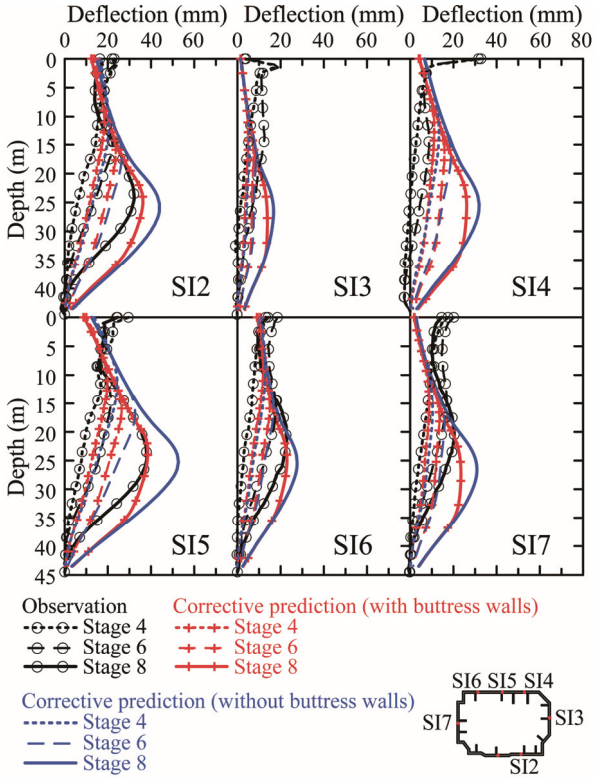

Fig. 11 Comparison of the diaphragm wall deflections at stages 4, 6 and 8 between the observation and the corrective prediction

to 8, the deflections of the diaphragm walls at SI2, SI5, SI6 and SI7 from the corrective prediction agreed well with those from the observation. The diaphragm wall deflections at SI3 from the observation and corrective prediction were smaller than other locations due to its position locating at the short excavation sides and subjected to corner effects. In addition, the deflection above the excavation surface at stage 6 from the corrective prediction was slightly smaller than that from the observation because construction material was stacked near SI3.

Figure 11 also shows that the maximum diaphragm wall deflections at stage 8 excavation at all inclinometers were smaller than the controlled value (50 mm). The predicted wall deflections were different from the empirical formula because the latter was established based on the normal construction. If the construction sequence used in the analysis was not under the normal condition, the empirical formula would deviate from those from the empirical formulae.

Based on the above comparisons, it can be found that the simulation used in the corrective prediction conformed to the actual excavation conditions. The corrective prediction could obtain reasonable results and also more consistent with the observation.

For evaluation of the efficiency of the installation of buttress walls, corrective prediction of the excavation with the assumption of no buttress walls installed was also performed and the results are also shown in Fig. 11. Similar to the preliminary prediction, the maximum diaphragm wall deflection occurred at SI5 where the δ_{hm} at stage 8 was 52.7 mm, slightly exceeding the controlled value. As described in the previous section, the *PSR* value of SI5 was estimated as 0.92. Therefor the $\delta_{hm,ps}$ could evaluate to be equal to 0.22% *H*, approximately lower limit of empirical formula (Eq. (2)). It should be noted that in the present case, dewatering alone actually can reduce the wall deflection. Under such a condition, buttress walls may not be necessary. However, the conclusion may not be applied to another case where geological condition and construction sequence are different. Numerical analysis is thus required to do design work.

As shows in Table 3, the *RRD* values at SI4, SI5 and SI6, located in the north of the excavation zone, were equal to 18.2%, 27.0% and 17.0%, respectively. The *RRD* values at SI2, in the south of the excavation zone, was 17.5%; at SI3, in the east, 17.4%; at SI7, in the west, 24.0%. The efficiency evaluated by the *RRD* values was similar to the first prediction.

6. DISCUSSION ON THE EFFICIENCY OF THE BUTTRESS WALLS

The predicted results in the previous sections, as displayed in Figs. 9, 11 and Table 3, show that the buttress walls could provide moderate reduction in the diaphragm wall deflection. The *RRD* values at SI5, in the north of the excavation, were relatively larger than that at SI6. That is because when the excavation was without buttress walls, the SI5 had a larger wall deflection or deflection potential. Once buttress walls were installed, the effects of buttress walls in reducing wall deflection mainly come from the surface friction of the buttress walls (Hsieh *et al*. 2013), the larger deflection potential could fully mobilize frictional resistance between the side surface of buttress walls and the adjacent soil. The buttress walls therefore had a better efficiency at SI5. In addition, The SI4 and SI6, in the north of the excavation, had a similar distance to an excavation corner and therefore have a similar $\delta_{hm,nobw}$. However, the *RRD* values at SI4 are larger than that at SI6, even larger than that at SI5 in the first prediction. The reason is that the wall deflection at SI4 had a relatively large $\delta_{hm,nobw}$ and longer buttress walls (Type C), as shown in Figs. 7 and 8, and therefore could provide better efficiency. Similar phenomena are also found at SI4 and SI2, in the north and south of excavation, respectively. The efficiency of buttress wall at SI4 was better than that at SI 2 because the former had a longer buttress wall than the latter. These results are consistent with the results in Hsieh *et al*. (2013).

The wall deflection at SI3 and SI7, located at the short excavation sides, had smaller $\delta_{hm,nobw}$. Since the wall at SI3 was subjected to corner effects, it had a smaller deflection, smaller deflection potential than that at SI7. Although both SI3 and SI7 had the same buttress wall length (Type B), the buttress walls at SI7 provided better efficiency.

The predicted results in the previous sections also show that the buttress walls installed in the studied project could reduce the diaphragm wall deflections, the *RRD* values with a range of 16.0% to 30.6% and 17.0% to 27.0% in the first prediction and corrective prediction, respectively. The reductions were not sufficiently large because the $\delta_{hm,nobw}$ from the preliminary prediction, empirical method and numerical analysis, at the design stage, was not significantly larger than the controlled value. The buttress wall was thus not designed with a significant length (Hsieh *et al*. 2013). Therefore for each excavation case, the required buttress wall length is not fixed and should be designed according to the difference between the predicted diaphragm wall deflections and the controlled value.

7. CONCLUSIONS

Buttress walls have been used as alternative auxiliary measures for protection of adjacent buildings during excavation in Taiwan. This study performs a case study regarding the design of an excavation with the installation of buttress walls. Based on the results of the observation and prediction, the soil and structure models and their parameters determination procedure for three-dimensional finite element method were established, and the simulation methods of the adjacent buildings and the lowered water level within the excavation zone due to diaphragm wall construction were suggested for reasonably predicting the overall diaphragm wall deflection of excavation with and without buttress walls. The efficiency of the buttress walls was also investigated.

The buttress walls could provide moderate efficiency in reducing the diaphragm wall deflection. When the diaphragm wall deflection of the excavation where was without any auxiliary measures was not very much larger than the controlled value, only a partial protection measure was needed. The buttress walls could be an appropriate measure for the consideration for quality and finance. A long buttress wall usually performances better than a short one. When the excavation was without buttress walls, the diaphragm wall had a larger deflection. Once buttress walls were installed, the larger deflection potential could fully mobilize frictional resistance between the side surface of buttress walls and the adjacent soil, the buttress walls generally had better efficiency. Therefore for each excavation case, the required buttress wall length is not fixed and should be designed according to the difference between the predicted diaphragm wall deflections and the controlled value.

In addition, the condition of ground water level within the excavation zone due to diaphragm wall construction and the simulation of the adjacent buildings should be appropriately taken into account in the analysis.

ACKNOWLEDGEMENTS

The authors acknowledge the support provided by the Ministry of Science and Technology in Taiwan via Grant No. MOST 103-2221-E-146 -004.

REFERENCES

ACI Committee 318 (1995). *Building Code Requirements for Structural Concrete (ACI 318-95) and Commentary (ACI 318R-95)*, American Concrete Institute (ACI), Farmington Hills, Mich.

Calvello, M. and Finno, R. (2004). "Selecting parameters to optimize in model calibration by inverse analysis." *Computer and Geotechnics*, **31**(5), 410–424.

Chen, S.L., Ho, C.T., Li, C.D., and Gui, M.W. (2011). "Efficiency of buttress walls in deep excavations." *Journal of GeoEngineering*, **6**(3), 145–156.

Deng, W.B. (2013). *The Effect of Buttress Walls on Wall Deflection in Deep Excavation*, Master's thesis, Department of Construction Engineering, National Taiwan University of Science and Technology, Taipei, Taiwan (in Chinese).

Gaba, A.R. (1990). "Jet grouting at Newton station." *Proceedings of the 10th Southeast Asia Geotechnical Conference*, Taipei, Taiwan, 77–79.

Hsieh, H.S. and Lu, L.C. (1999). "A note on the analysis and design of diaphragm wall with buttresses." *Sino-Geotechnics*, **76**, 39–50.

Hsieh, H.S., Wang, C.C., and Ou, C.Y. (2003). "Used of jet grouting to limit diaphragm wall displacement of deep excavation." *Journal of Geotechnical and Geoenvironmental Engineering*, ASCE, **129**(2), 146–157.

Hsieh, P.G. (1993). *Consideration on Anisotropic Behavior in Finite Element Analysis of Deep Excavation*, Master's thesis, Department of Construction Engineering, National Taiwan Institute of Technology, Taipei, Taiwan (in Chinese).

Hsieh, P.G., Deng, W.B., and Ou, C.Y. (2013). "A study of diaphragm wall movements restrained by buttress walls." *Proceedings of the 2013 Cross-Strait Seminar on Ground Engineering*, Taipei, Taiwan, 197–204 (in Chinese).

Hsieh, P.G. and Ou, C.Y. (1998). "Shape of ground surface settlement profiles caused by excavation." *Canadian Geotechnical Journal*, **35**(6), 1004–1017.

Hsieh, P.G., Ou, C.Y., and Lin, Y.L. (2013). "Three dimensional numerical analysis of deep excavations with cross walls." *Acta Geotechnica*, **8**(1), 33–48.

Huang, C.T., Lin, Y.K., Kao, T.C., and Moh, Z.C. (1987). "Geotechnical engineering mapping of the Taipei city." *Proceedings of the 9th Southeast Asia Geotechnical Conference*, Bangkok, Thailand, **1**, 3-109–3-120.

Hwang, R.N., Moh, Z.C., and Wang, C.H. (2007). "Performance of wall systems during excavation for Core Pacific City." *Journal of GeoEngineering*, TGS, **2**(2), 53–60.

Jaky, J. (1944). "The coefficient of earth pressure at rest." *Journal of the Society of Hungarian Architects and Engineers*, **78**(22), 355–358.

Khoiri, M. and Ou, C.Y. (2013). "Evaluation of deformation parameter for deep excavation in sand through case histories." *Computers and Geotechnics*, **47**(1), 57–67.

Ladd, C.C., Foott, R., Ishihara, K., Schlosser, F., and Poulos, H.G. (1977). "Stress-deformation and strength characteristics." *Proceedings of the 9th International Conference on Soil Mechanics and Foundation Engineering*, Tokyo, Japan, **2**, 421–494.

Lim, A., Ou, C.Y., and Hsieh, P.G. (2010). "Evaluation of clay constitutive models for analysis of deep excavation under undrained conditions." *Journal of GeoEngineering*, TGS, **5**(1), 9–20.

Lin, D.G. and Woo, S.M. (2007). "Three dimensional analyses of deep excavation in Taipei 101 construction project." *Journal of GeoEngineering*, TGS, **2**(1), 29–41.

Liu, G.B., Ng, C.W.W.M., and Wang, Z.W. (2005). "Observed performance of a deep multistrutted excavation in Shanghai soft clays." *Journal of Geotechnical and Geoenvironmental Engineering*, ASCE, **131**(8), 1004–1013.

Ou, C.Y. (2006). *Deep Excavation: Theory and Practice*, Taylor & Francis.

Ou, C.Y., Chiou, D.C., and Wu, T.S. (1996). "Three-dimensional finite element analysis of deep excavations." *Journal of Geotechnical Engineering*, ASCE, **122**(5), 337–345.

Ou, C.Y., Hsieh, P.G., and Chiou, D.C. (1993). "Characteristics of ground surface settlement during excavation." *Canadian Geotechnical Journal*, **30**(5), 758–767.

Ou, C.Y., Hsieh, P.G., and Lin, Y.L. (2011). "Performance of excavations with cross walls." *Journal of Geotechnical and Geoenvironmental Engineering*, ASCE, **137**(1), 94–104.

Parashar, S., Mitchell, R., Hee, M.W., Sanmugnathan, D., Sloan, E., and Nicholson, G. (2007). "Performance monitoring of deep excavation at Changi WRP project," *Proceedings of the 7th International Symposium on Field Measurements in Geomechanics*, Singapore, 1–12.

PLAXIS (2013). *PLAXIS 3D Computer Software*. Delft, Netherlands, PLAXIS.

Schanz, T., Vermeer, P.A., and Bonnier, P.G. (1999). "The hardening soil model: Formulation and verification." *Beyond 2000 in Computational Geotechnics*, Rotterdam, 281–290.

Taiwan Geotechnical Society (2001). *Design Specification the Foundation of the Building*, Taiwan Geotechnical Society, TGS, Taiwan.

Wong, K.S., Wong, I.H., and Broms, B.B. (1987). "Methods of improving the stability of deep excavations in soft clay." *Proceedings of the 8th Asian Regional Conference on Soil Mechanics and Foundation Engineering*, Kyoto, Japan, 321–324.